PCCP

Accepted Manuscript

ROYAL SOCIETY OF CHEMISTRY

www.rsc.org/pccp

Journal Name

RSCPublishing

ARTICLE

Enhanced electrochromic properties of polypyrrole/indigo carmine/gold nanoparticles nanocomposite

Cite this: DOI: 10.1039/x0xx00000x

Received 00th January 2012,
Accepted 00th January 2012

DOI: 10.1039/x0xx00000x

www.rsc.org/

L.F. Loguercio,[a] C.C. Alves,[a] A. Thesing,[a] J. Ferreira[b]*

Indigo carmine doped polypyrrole embedded with gold nanoparticles nanocomposite ($PPy/IC/Au_{nanop}$) was synthesized by *insitu* electrochemical polymerization of polypyrrole in the presence of $HAuCl_4$. The nanocomposite was characterized by *in situ* spectroelectrochemical experiments to study the effect of embedded gold nanoparticles on the electrochromic properties of the material. The results show the formation of a nanocomposite presenting enhanced electrochromic and optical properties, higher electroactivity and 10% lower band-gap energies. The $PPy/IC/Au_{nanop}$ presented a two-fold increase in optical contrast when compared to PPy/IC, in addition to better optical stability.

Introduction

The understanding of physical and chemical properties of electrochromic materials has attracted the interest of academy and industry, due to their fundamental spectroelectrochemical properties and wide range of applications including controllable light-transmissive devices for optical information and storage, sunroofs, visors, anti-glare car rear-view mirrors, protective eyewear and "smart windows".[1-8]

Many classes of materials present electrochromic behavior, such as transition metal oxides, buckminsterfullerene, polyoxometalates, metallopolymers, phthalocyanines and conducting polymers.[1,6-9] The latter have received increasing attention in the last two decades, due to their printable properties and tunable nature of HOMO and LUMO, resulting in tunable optical and electrical properties which are dependent of organic or inorganic dopants.[1,10-19]

The charges generated in conducting polymers are stabilized by either p-doping or n-doping. However, p-doped conducting polymers are more interesting for application on electrochromic devices due to their higher stability, when compared to n-doped polymers.[1] Polypyrrole (PPy) is one of the most studied p-doped polymers, presenting good environmental stability, high electrical conductivity, easy synthesis by either electrochemical or chemical methods, film forming ability and biocompatibility.[20-22]

In principle, any anion can act as a dopant for PPy, however, previous studies have demonstrated that using large electroactive organic molecules, result in PPy films with better stability, electron transfer and electrochromic properties, than using standard inorganic anions (e. g. ClO_4^-).[17,23-25]

Indigo carmine (IC) is an interesting molecule to use as dopant for PPy, presenting well-known redox mechanism, high extinction coefficient, dianionic character, allowing to form smoother PPy films, with more homogeneous surface, in addition to improve the optical properties of PPy films.[23-28] According to the literature, indigo carmine molecules act as a bridge or nanochannel between PPy chains, inducing a certain degree of order in PPy/IC film, stabilizing the polymer on quinoid form.[15,29] This configuration facilitates the ionic changes on electrochemical processes, leading to improvements of electrochromic properties.[29-31]

Recently, the incorporation of metallic nanoparticles into polypyrrole have resulted in enhanced electrical and electrochemical properties, improving conductivity, robustness, stability and electrocatalytic activity.[32-35] Taking into account the results obtained from studies on PPy/IC and the effect of metallic nanoparticles on the optical properties of organic molecules, one should expect an interesting interaction between metallic nanoparticles and conducting polymers, which could result in improved electrochromic properties.

In this work, we have studied the effect of gold nanoparticles on the electrochromic properties of indigo carmine doped polypyrrole. Thin films of nanocomposite were characterized by Scanning Electron Microscopy (SEM), Energy Dispersive X-ray analysis (EDX), high-resolution SEM,

Transmission Electron Microscopy (TEM), Fourier Transform Infrared - Attenuated Total Reflectance (FTIR), cyclic voltammetry and classical electrochromic measurements.

Experimental

Materials

Pyrrole (Aldrich) was double distilled and stored under N_2 at *ca.* 4 °C. Indigo carmine, sodium citrate, potassium chloride and $HAuCl_4$ (Aldrich) were used as received. All solutions were prepared with ultrapure water (Milli-Q).

Apparatus

Electropolymerization

$PPy/IC/Au_{nanop}$ films (1 cm^2) were electropolymerized during three voltammetric cycles from -0.3 to +1.3 V at scan rate of 30 mV s^{-1} in a three-electrode cell, using a galvanostat/potentiostat Autolab 302N. Fluorine doped tin oxide (FTO, Solaronix, 15 $\Omega.cm^{-2}$) was used as working electrode, a platinum wire as counter electrode and Ag/AgCl as the reference electrode. The synthesis solution was 0.1 mol L^{-1} pyrrole, 5.0 mmol L^{-1} IC and 1 mol L^{-1} $HAuCl_4$ solution. For comparison, PPy was also electropolymerized in the absence of $HAuCl_4$ (PPy/IC). The temperature during synthesis was controlled with a thermostat SBS at 10 °C due to better degree of order in PPy/IC films in this temperature.[15,34] For optical and spectroelectrochemical characterization, PPy films were also synthesized at 25 °C. These temperatures are within the optimum temperature range (from 10 to 30 °C) to form polypyrrole films with high conductivity.[36]

Characterization

Cyclic voltammetry experiments were performed within a potential range from – 1.0 to + 1.0 V, during 6 cycles at scan rate of 50 mV s^{-1}. The electrolyte was 0.1 mol L^{-1} KCl solution. Infrared spectroscopy was carried out in Attenuated Total Reflectance mode (FTIR-ATR) using a Bruker equipment, model Alpha-P. Morphological characterization was performed by Scanning Electron Microscopy using an EVO50 – Carl Zeiss microscope at 15 kV with Energy Dispersive X-ray analysis, High Resolution SEM with a JEOL-7500F at 5 kV and Transmission Electron Microscopy with a JEOL JEM 1200 ExII. *In situ* UV-Vis spectroelectrochemical experiments were carried out using a PerkinElmer Lambda 25 spectrophotometer and a galvanostat/potentiostat Autolab 302N. A quartz cuvette was used for a two-electrode configuration cell. Double step potentials of - 0.6 and + 0.4 V were applied during the electrochromic characterization for a period of 80 s. Time domain measurements were carried out by collecting one spectra each 0.5 s.[15,29]

Results and discussion

Structural characterization

Fig. 1 shows FTIR spectra of pristine indigo carmine, PPy/IC and $PPy/IC/Au_{nanop}$. One can observe the vibrational modes characteristic of PPy at 1527 cm^{-1}, assigned to N-H stretch, at 1010 cm^{-1} and 960 cm^{-1} assigned to angular deformations in plane of C-H, N-H and C-N-C bonds in the pyrrole ring.[37-40] The presence of IC molecules in PPy matrix is characterized by C=O group and sulphonate anion vibrational mode at 1630 and 1026 cm^{-1}, C–O, C-N-C and S-O stretching at 1094 cm^{-1}, 900 cm^{-1} and 843 cm^{-1}, respectively.[19,41-43] These vibrational modes are shifted in PPy/IC and $PPy/IC/Au_{nanop}$, suggesting chemical interactions between polypyrrole, indigo carmine and/or gold.

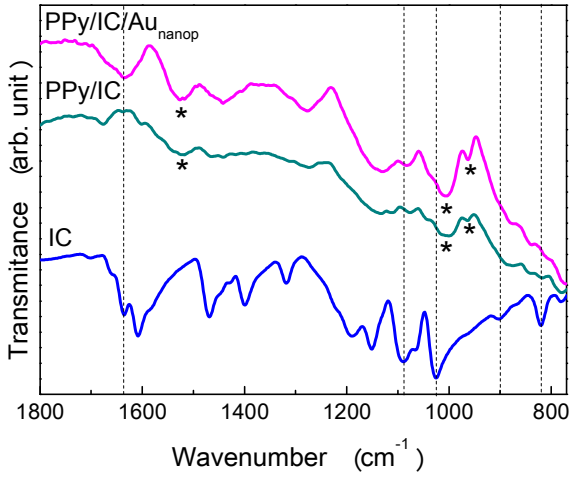

Fig. 1 FTIR-ATR spectra from PPy/IC; $PPy/IC/Au_{nanop}$ films and pristine IC dye. *Vibrational modes assigned to PPy.

During electrochemical polymerization, the pyrrole monomer is oxidized forming a radical cation which can react either with another radical cation or a monomer. The cation formation is energetically favoured in the presence of counter ions such as IC molecules, acting as dopant due to their negative charges. At the same time, gold ions are reduced on the working electrode surface. Similar to previous studies of PPy-silver nanocomposites, the electrodeposited Au nanoparticles may act as adsorption centers for oxidized monomers and oligomers of pyrrole (cations) due to a large number of electrons around the gold atoms (Fig. 2).[44]

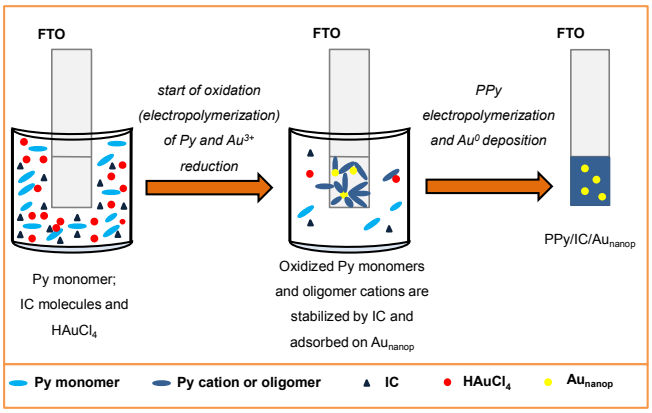

Fig. 2 Scheme illustrating the one-step electropolymerization of $PPy/IC/Au_{nanop}$.

The growth of nanoparticles during the pyrrole polymerization may result in: i) formation of HOMO and LUMO with

topologically similar phase relationships in the interaction regions;[45] ii) changes in polaronic/bipolaronic levels in the band gap[58] and iii) new energy levels in the band gap,[46-48] favoring charge separation.

Morphological characterization

Fig. 3 a and b show SEM images from PPy/IC and PPy/IC/Au_{nanop} films. Both PPy films presented the formation of a homogeneous surface with small globules. The temperature of synthesis (SEM not shown) and the presence of gold nanoparticles seems not to affect significantly the morphology of the nanocomposite. These observations suggest the dopant as the main responsible for the morphological properties of the film.

Fig. 3 b1 and b2 show the EDX mapping for sulphur (element present in indigo carmine) and gold in the PPy/IC/Au_{nanop} film. In the conditions used in this work, the presence of gold does not affect the distribution of dopant in the PPy matrix and a homogenous distribution of both gold and dopant is observed.

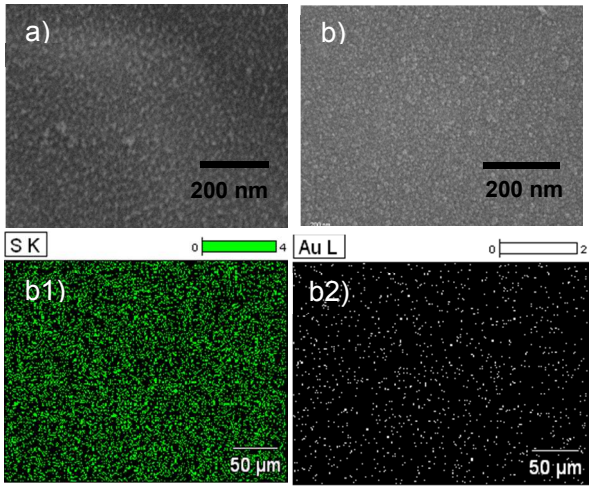

Fig. 3 SEM images and EDX mapping for a) PPy/IC and b) Ppy/IC Au_{nanop} synthesized at 10 °C. b1) EDX mapping for sulphur (present in indigo carmine molecular structure). b2) EDX mapping for gold (present in PPy/IC/Au_{nanop} films).

The TEM image (Fig. 4a) of PPy/IC/Au_{nanop} shows the presence of gold nanoparticles embedded within the film (arrows indicate the nanoparticles), which corroborates the EDX mapping (Fig. 3). TEM as well as high-resolution SEM images of the nanocomposite (Fig. 4b) show spherical gold nanoparticles presenting average diameter of 10 nm, in addition to the formation of aggregates.

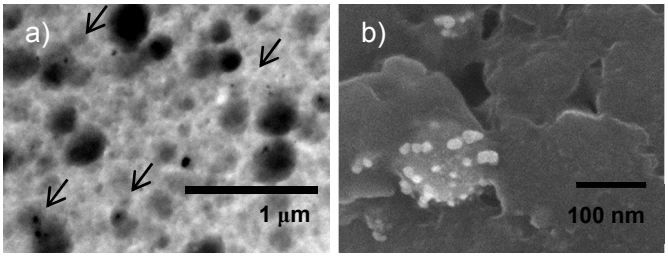

Fig. 4 a) TEM and b) high-magnification SEM images of the PPy/IC/Au_{nanop} nanocomposite.

Electrochemical characterization

Fig. 5 shows the voltammograms of PPy/IC and PPy/IC/Au_{nanop}. One can observe slightly shifts of the redox potentials after incorporating gold nanoparticles into the film. PPy/IC presents anodic and cathodic potentials at ca. 0.28 V and - 0.15 V, respectively. Meanwhile, PPy/IC/Au_{nanop} displays anodic and cathodic peaks at ca. 0.44 V and - 0.23 V. In addition, PPy/IC/Au_{nanop} displays a couple of oxidation and reduction waves that could be related to a process involving a new bond between PPy, Au nanoparticle and electrolyte.[44] For PPy/IC, the peak-to-peak separation (ΔE_p)and formal potential [($E_a + E_c / 2$)] was calculated as 0.43 V and 0.06 V. For PPy/IC/Au_{nanop}, ΔE_p was found as 0.67 V, and formal potential 0.10 V. These results suggest a facilitated charge transport in both polymeric films.[34] The ratio |Ia|/|Ic| calculated for both voltammograms is close to one, indicating a good reversibility for the systems.

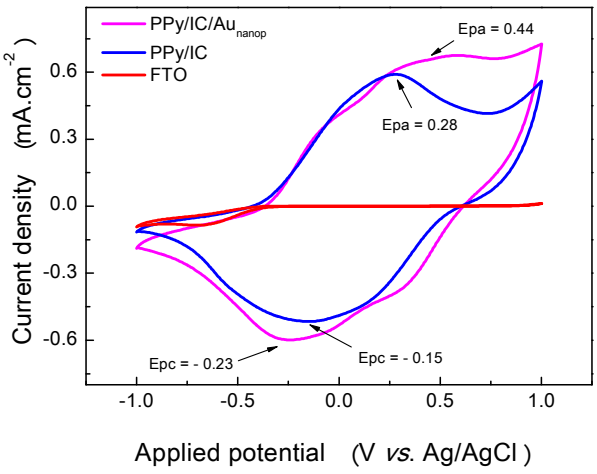

Fig. 5 Voltammograms on PPy/IC and PPy/IC/Au_{nanop} synthesized at 10 °C in 0.1 $molL^{-1}$ KCl solution at scan rate of 50 mVs^{-1}. Fifth cycle.

The wider voltammetric wave and the positive shift of the anodic potential observed for PPy/IC/Au_{nanop} suggests chemical interactions between chain segments of PPy and the gold nanoparticles, as earlier suggested in the FTIR spectra (Fig. 1).[15,49-52] The nanocomposite presents higher current and charge densities than PPy/IC (*ca.* 19% increase in charge density), synthesized under the same conditions. The presence of gold nanoparticles may avoid the charge motion limitation due to chain length, facilitating electrons transfer, improving the conduction by "hopping" due to their good conductivity,[53] increasing the conduction path and allowing a charge accumulation on the modified electrode surface.

Optical characterization

In addition to the effect of gold nanoparticles, the effect of synthesis temperature on the optical properties of PPy was evaluated by synthesizing the films at 10 °C and 25 °C. By comparing the UV-Vis absorption spectra of PPy/IC and PPy/IC/Au_{nanop} (Fig. 6), one can observe a redshift of the maximum absorption band (electronic transition for oxidized PPy)[37] due to the presence of gold nanoparticles, for both synthesis temperature. According to the literature, this redshift can be associated to structural changes in the polymer matrix, leading to higher molecular ordering, caused by the dye molecules.[54]

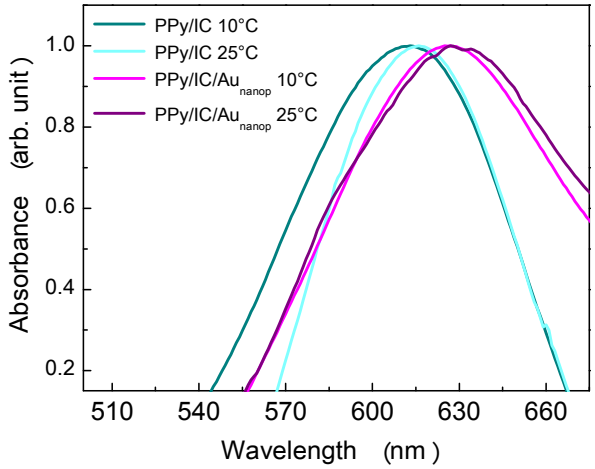

Fig. 6. Absorption UV-Vis spectra of PPy/IC and PPy/IC/Au_{nanop} synthesized at 10 °C and 25°C.

In order to further evaluate the effect of gold nanoparticles on the electrical and optical properties of the polymeric film we have calculated the energy gap (E_{gap}) by Tauc equation:[55]

$$[\alpha h\nu]^n = K\left(h\nu - E_g\right) \quad (1)$$

where n represents the nature of the transition, K is a constant; $h\nu$ is the photon energy and α is the absorption coefficient obtained from the absorbance (A) and thickness of the sample (d):[56]

$$\alpha(\nu) = 2.303\,A(\nu)/d \quad (2)$$

by extrapolating the linear part of $(\alpha h\nu)^2$ or $(\alpha h\nu)^{1/2}$ vs. $h\nu$ to $\alpha = 0$, one can obtain the E_{gap} values.

For a direct transition ($n = 2$), Equation 1 becomes:

$$[\alpha h\nu]^2 = K\,(h\nu - E_g) \quad (3)$$

For an indirect transition ($n = 1/2$), Equation 1 becomes:

$$[\alpha h\nu]^{1/2} = K\,(h\nu - E_g) \quad (4)$$

Table 1 shows the estimated direct and indirect band-gap energies obtained through $(\alpha h\nu)^2$ and $(\alpha h\nu)^{1/2}$ versus $h\nu$ plots (not shown), respectively.[57]

Table 1. Direct and indirect band-gap energies of the polymeric films synthesized at different temperatures.

Film	E_{gap}^{direct} (eV)	$E_{gap}^{indirect}$ (eV)
PPy/IC 10°C	1.84	1.68
PPy/IC 25°C	1.83	1.66
PPy/Au_{nanop} 10°C	1.68	1.50
PPy/Au_{nanop} 25°C	1.66	1.43

By comparing the results presented in Table 1 to the literature, one can observe that the presence of IC dopant allows for the synthesis of PPy presenting lower direct energy band gaps than using inorganic ions, which can be associated to higher molecular ordering, caused by IC molecules.[15,54,58-60] In addition, a very interesting result is the effect of gold nanoparticles resulting in a decrease of both direct and indirect energy gap. Embedding gold nanoparticles into PPy matrix seems to have a more significant effect on the indirect transition, resulting in a decrease in E_{gap} up to 14%. There results strongly suggest that the metallic nanoparticles promote structural changes in the polymer, improving molecular ordering, and also affects the band gap of PPy resulting in a redshift of the absorption band.

The synthesis temperature seems to have no effect on the band-gap energies of PPy. Only the nanocomposite presented a 5% decrease of indirect E_{gap} with the increase of temperature. The hypothesis for this behavior is based on a kinetic effect, where the increase of temperature lead to a higher amount of gold nanoparticles dispersed in the PPy matrix due to a higher nucleation / growth rate. Nevertheless, it is important to highlight that the polymer films synthesized at lower temperatures are thinner, present better adherence to the substrate, in addition to higher level of chain organization.[15] All these characteristic are important for the electrochromic properties of the film.[5,10]

Electrochromic characterization

Optical contrast (Δ%T)

The optical contrast (chromatic contrast) is an important property to evaluate the nanocomposite electrochromic behaviour, as it is a measure of the transmittance variation (Δ%T) at a specified wavelength. In this work, we have used -0.6 V and + 0.4 V as redox potentials and have monitored the optical contrast at 700 nm, in order to compare this study to other works in literature.[12,15,29] Considering the

polaron/bipolaron model, under positive applied potential the polaron formation is evidenced by the absorption band at ca. 530 nm and the bipolaron by the absorption band at ca. 700 nm.

According to Fig. 7, the synthesis temperature affects the optical contrast as higher values was achieved for PPy/IC and PPy/IC/Au_{nanop} synthesized at 10 °C (Table 2). The lower synthesis temperature allows better chain ordering, higher adherence to the substrate and lower thickness, allowing better charge transport during the doping/undoping process.[1,15] In addition, PPy/IC/Au_{nanop} always presented higher optical contrast than PPy/IC, suggesting the dependence of the electrochromic properties with the presence of gold nanoparticles. These behaviours were observed for both visible (530 nm) and NIR (700 nm) regions of electromagnetic spectrum.

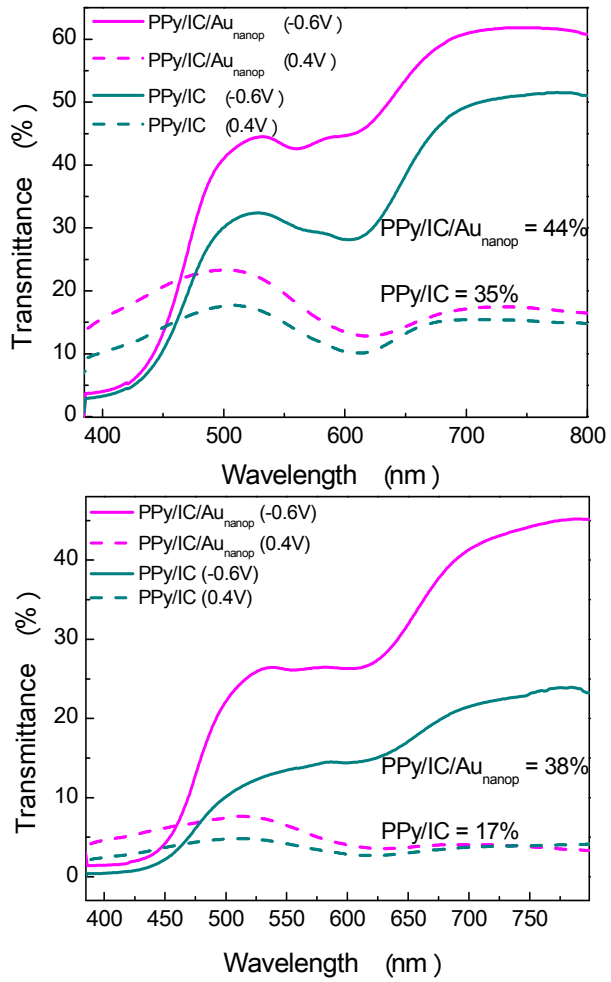

Fig. 7. Optical contrast of PPy/IC and PPy/IC/Au_{nanop} synthesized at 10 °C (top) and 25 °C (bottom). The redox potentials (- 0.6 V and 0.4 V) were applied for 80 s.

Table 2. Optical contrast at 530 and 700 nm of PPy/IC and PPy/IC/Au_{nanop} synthesized at different temperatures.

Material	Synthesis Temperature (°C)	Δ%T(λnm)
PPy/IC	10	35 (700)
PPy/IC	10	15 (530)
PPy/IC	25	17 (700)
PPy/IC	25	7 (530)
PPy/IC/Au_{nanop}	10	44 (700)
PPy/IC/Au_{nanop}	10	22 (530)
PPy/IC/Au_{nanop}	25	38 (700)
PPy/IC/Au_{nanop}	25	19 (530)

Table 3 shows the optical contrast from different electrochromic materials based on conducting polymers. One can observe that PPy/IC/Au_{nanop} presents larger optical contrast than all other materials which do not present metallic nanoparticles. Therefore there is an interaction between gold nanoparticles and PPy, which result in improved optical properties.

Table 3. Optical contrast of different conducting polymers based materials.

Material	Δ%T(λnm)	Ref.
PPy/RB	41 (795)	12
PPy/DR	23 (795)	12
PPy/DS/IC	37 (700)	15
PPy/ECR	27 (800)	29
PANI/WO_3	19 (633)	61
P(DTTP-*co*-EDOT) /EDOT	20 (487)	62
PPy/IC	35 (700)	*
	15 (530)	*
PPy/IC/Au_{nanop}	44 (700)	*
	22 (530)	*

* presented in this work

WRITE-ERASE EFFICIENCY

The electrochromic efficiency (η) or write-erase efficiency was calculated by Equation 5, which relates the optical contrast (Δ%T at 700 nm) with the total charge (Q) of oxidation or reduction, identified as anodic and cathodic efficiencies, respectively. These charges are determined from the integration of the chronoamperograms plots (current *vs.* time, not shown). The anodic (Q_a) and cathodic charge (Q_c) allows for calculating the oxidation (darkening) and reduction (bleaching) electrochromic efficiencies, respectively.

$$\eta(\lambda) = (\Delta\%T)/Q \quad (5)$$

According to the results showed in Table 3, films synthesized at 10 °C presented higher electrochromic efficiencies. In addition, the cathodic efficiency (η_c) was always higher than the anodic (η_a) probably due to a higher chain ordering (intramolecular interaction: π-packing) at the reduced state, favoring mass motion at the polymer/electrolyte

interface. At the oxidative state, local geometric distortions of polymeric chains does not favor mass motion at the interface.[15] The fact that $Q_a > Q_c$ indicates an uncompleted reduction process at this potential.

Table 4. Electrochromic efficiencies of PPy/IC/Au_{nanop} synthesized at 10 and 25 °C.

Film	Δ%T	Q_a^*	Q_c^*	$\eta_a^\#$	$\eta_c^\#$
PPy/IC/Au_{nanop} 10°C	44	3.4	1.5	12.9	29.3
PPy/IC/Au_{nanop} 25°C	38	7.7	5.0	4.4	6.8

*mC s^{-1},#$_s$ mC^{-1}

Response time

The electrochromic response time or optic response time is the shortest time required for a material to reach minim
um or maximum transmittance under external voltage. The response time is dependent on temperature, dopant concentration, polymer film thickness and method of synthesis.[1,10] Fig. 8 shows the *in situ* UV-Vis spectroelectrochemical analysis of the films synthesized at 10 °C, as they presented better optical contrast and electrochromic efficiency. PPy/IC and PPy/IC/Au_{nanop} presented similar cathodic (*ca.* 12 and 10 s) and anodic response time (3 and 4 s), respectively. The nanocomposite, reached higher values for transparency and opacity, which corroborates the results presented in Fig. 7.

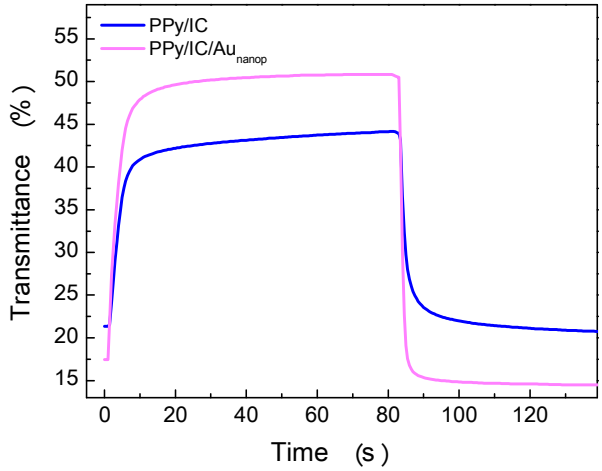

Fig. 8. Response time to optical contrast at 700 nm of PPy/IC and PPy/IC/Au_{nanop} synthesized at 10 °C. The redox potentials (- 0.6 V and 0.4 V) were applied for 80 s.

Optical stability

The plots presented in Fig. 9 show that PPy/IC film presents a dramatically drop in optical contrast reaching around 2% after the cycling. On the other hand, the nanocomposite presented fairly stable optical contrast during charge/discharge cycling.

It is well discussed in the literature that polaron and bipolaron states are associated to intermediary energy levels within the electronic band gap region of conducting polymers due to oxidation.[63,64] The ionized states are stabilized by geometrical chain distortion, once the polymeric chain has to accommodate the charges created by the oxidation process. The accommodation of these extra charges involves conformational and structural changes, which might lead to a leaching of dopant during the doping/undoping process, affecting the stability of optical contrast as observed for PPy/IC. In the nanocomposite, the more stable behavior might be related to adsorption of indigo carmine on the nanoparticles, remaining trapped into the film during the doping/undoping cycling.

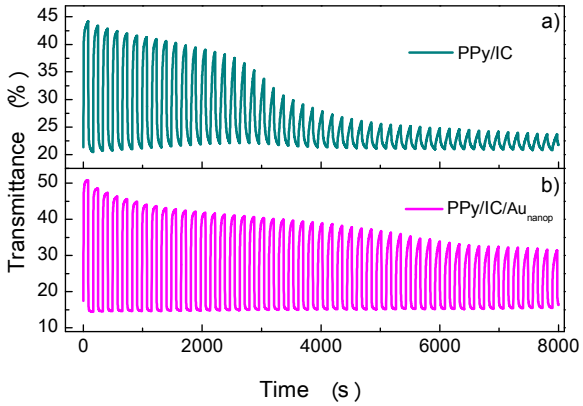

Fig. 9. Transmittance as a function of time during charge/discharge cycles on a) PPy/IC and b) PPy/IC/Au_{nanop} synthetized at 10 °C

Conclusions

We demonstrated the enhancement of electrochromic properties of a dye doped polypyrrole film, provided by growing gold nanoparticles into the polypyrrole matrix during electrochemical polymerization. This one-step procedure allows decreasing the energy-band gap, which is well known for modulating optical and electrical properties of conducting polymers. The simple electrochemical polymerization method used in this work can be extended to investigate a wide range of dye doped conducting polymers nanocomposites, leading to further improvements on the development of flexible and low cost electrochromic devices.

Acknowledgements

The authors gratefully acknowledge funding supports, scholarships and fellowship for this work from *Fundação de Amparo à Pesquisa do Estado do Rio Grande do Sul* (FAPERGS), *Conselho Nacional de Desenvolvimento Científico e Tecnológico* (CNPq – Brazil) and *Coordenação de Aperfeiçoamento de Pessoal de Nível Superior* (CAPES). They are thankful to Multidisciplinary Center for Development of Ceramic Materials (CDCM) from *Universidade Estadual Paulista* (UNESP) for the high-magnification SEM images.

Notes and references

[a]Centro de Ciências Químicas, Farmacêuticas e de Alimentos, Universidade Federal de Pelotas, C. P. 354, 96010-900, Pelotas, RS, Brazil.
[b]Instituto de Química, Universidade Federal do Rio Grande do Sul, C. P. 15003, 91501–970, Porto Alegre, RS, Brazil.
*e-mail: jacqueline.ferreira@ufrgs.br.

1 P. R. Somani and S. Radhakrishnan, *Mater. Chem. Phys.*, 2002, **77**, 117.
2 J. Ferreira, A. G. Brolo and E. M. Girotto, *Electrochim. Acta*, 2011, **56**, 3101.
3 P. M. S. Monk, R. J. Mortimer and D. R. Rosseinsky, Electrochromism and electrochromic devices, 1nd ed, 2007, Cambrigde University Press (New York), p 312.
4 C. G. Granqvist, Handbook of Inorganic Electrochromic Materials, 1nd ed, 1995, Elsevier Science B.V. (Amsterdam), p 633.
5 R. J. Mortimer, *Chem. Soc. Rev.,*1997, **26**, 147.
6 M. J. L. Santos, A. F. Rubira, R. M. Pontes, E. A. Basso and E. M. Girotto, *J. Solid State Electrochem.*, 2006, **10**, 117.
7 J. Matsui, R. Kikuchi and T. Miyashita, *J. Am. Chem. Soc.*, 2014, **136**, 842.
8 S-M. Wang, L. Liu, W-L. Shen and E-B. Wang, *Electrochim. Acta*, 2013, **113**, 240.
9 M. Arici, C. Bozoglu, A. Erdogmus, A. L. Ugur and A. Koca, *Electrochim. Acta*, 2013, **113**, 668.
10 P. M. Beaujuge and J. R. Reynolds, *Chem. Rev.,*2010, **110**, 268.
11 E. Oguzhan, H. Bilgili, F. B. Koyuncu and E. Ozdemir, *Polymer*, 2013, **54**, 6283.
12 J. Ferreira, M. J. L. Santos, R. Matos, O. P. Ferreira, A. F. Rubira and E. M. Girotto, *J. Electroanal. Chem.*, 2006, **591**, 27.
13 J. L. Bredas, W. R. Salaneck, and G. Wegner, Organic materials for electronics: conjugated polymer interfaces with metals and semiconductors, 1nd ed, 1994, Elsevier (Amsterdam), p 133.
14 J. Ferreira and E. M. Girotto, *J. Braz. Chem. Soc.*, 2010, **21**, 312.
15 E. M. Girotto and M.-A. De Paoli, *Adv. Mater.*, 1998, **10**, 790.
16 J. Roncali, *Chem Rev*, 1992, **92**, 711.
17 J. Ferreira and E. M. Girotto, *Sens. Actuat. B*, 2009, **137**, 426.
18 R. Doyle, C. B. Breslin, O. Power and A. D. Rooney, *Electroanalysis,* 2012, **24**, 293.
19 I. Sultona, M. M. Rahman, J. Wang, C. Wang, G. G. Wallace and H-K. Liu, *Solid State Ionics*, 2012, **215**, 29.
20 T. A. Skothein, Handbook of conducting polymers, v. 2, 1986, Marcel Dekker (New York),p 825.
21 H. Gerischer and C. W. Tobias, Advances in electrochemical science and engineering, 1nd ed, 1990, VCH Publishers (New York), p 205.
22 E. M. Geniès, G. Bidan and A. F. Diaz, *J. Electroanal. Chem.*, 1983, **149**, 101.
23 W. Zhang, S. Song and S. Dong, *J. Inorg. Biochem.*, 1990, **40**, 189.
24 J. Hazarika and A. Kumar, *Synthetic Met*, 2013, **175**, 162.
25 Z. Gao, A. Lewenstam and A. Ivaska, *Electrochim. Acta*, 1994, **39**, 755.
26 Y. Li and S. Dong, *J. Electroanal. Chem.*, 1993, **348**, 181.
27 B. Shen, M. Olbrich-Stock, J. Posdorfer and R. N. Schindler, Z *Phys. Chem.*, 1991, **173**, 251.
28 J. Fabian and H. Hartman, Light absorption of organic colorants, 1976, Springer-Verlag (Berlin), p 195.
29 F. Tavoli and N. Alizadeh, *J Electroanal Chem,* 2014, **720**, 122.
30 P. Somani and S. Radhakrishnam, *Chem. Phys. Lett.,* 1998, **292**, 222.
31 M-A. De Paoli, G. C. Miceli, E. M. Girotto and W. A. Gazoti, *Electrochim. Acta,* 1999, **44**, 2991.
32 W. Chena, C. Ming Li, P. Chena and C. Q. Sun, *Electrochim. Acta.*, 2007, **52**, 2845.
33 S. Ye, L. Fang and Y. Lu, *Phys. Chem. Chem. Phys.*, 2009, **11**, 2480.
34 S. Singh, D. V. S. Jain and M. L. Singla, *Anal. Methods*, 2013, **5**, 1024.
35 D. W. Hatchett and M. Josowicz, *Chem. Rev.*, 2008, **108**, 746.
36 A. Kassim, Z. B. Basar and H. N. M. E. Mahmud, *Proc. Indian Acad. Sci.*, 2002, **114**, 155.
37 E. Hakansson, T. Lin, H. Wang and A. Kaynak, *Synthetic Met.*, 2006, **156**, 1194.
38 B. Tian, G. Zerbi, *J. Chem. Phys.,* 1990, **92**, 3886.
39 R. Kosti, D. Rakovi, S. A. Stepanyan, I. E. Davidora and L. A. Gribov, *J. Chem. Phys.*, 1995, **102**, 3104.
40 J. Hazarika and A. Kumar, *Synthetic Met.*, 2013, **175**, 155.
41 Ch. C. Rajeev, K. S. Brijesh, *Spectrochim. Acta A,*2014, **124**, 138.
42 J. E. Rode, E. D. Raczyńska, E. Cz. Gornicka, J. Dobrowolski, *J. Mol. Struct*. 2005; **749**: 51.
43 Y. Han, M. Shen, J. Zhu, Y. Wu, X. Zhang, *Polym Composite*, 2013, 989.

44 K. E. Hnida, R. P. Socha and G. D. Sulka, *J. Phys. Chem. C*, 2013, **117**, 19382.
45 D. K. Seo and R. Hoffman, *Theor. Chem. Acc.*, 1999, **102**, 23.
46 C. Zeng, W. Shen, X. Xie and Ming Li, *Polym. Sci. Ser. A*, 2010, **52**, 1355.
47 L. B. Scaffardi and J. O. Tocho, *Nanotechnology*, 2006, **17**, 1309.
48 T. A. Skotheim and J. R. Reynolds, Conjugated polymer: processing and applications, in Handbook of conducting polymer, 3nd ed, 1949, CRC Press (USA), p 15.
49 M. J. L. Santos and E. M. Girotto, *J. Braz. Chem. Soc.*, 2009, **20**, 229.
50 E. M. Girotto, N. Camaioni, G. Casalbore-Miceli, M-A. de Paoli, A. M. Fichera and M. C. Gallazzi, *J. App. Electrochem.*, 2001, **31**, 335.
51 E. M. Girotto, G. Casalbore-Miceli, N. Camaioni, M-A. De Paoli, A. M. Fichera, L. Belobrzeckaja and M. C. Gallazzi, *J. Mater. Chem.*, 2001, **11**, 1072.
52 G. Casalbore-Miceli, N. Camaioni, V. Fattori, A. M. Fichera, M. C. Gallazzi, A. Geri, E. M. Girotto and G. Giro, *Synthetic Met.*, 2001, **121**, 1575.
53 K. Gupta, P. C. Jana and A. K. Meikap, *Synthetic Met,* 2010, **160**, 1566.
54 Y. Li, *Electrochim Acta*, 1997, **42**, 203.
55 M. M. Abdi, H. N. M. E. Mahmud, L. C. Abdullah, A. Kassim, M. Z. Ab Rahman and J. L. Y. Chyi, *Chin. J. Polym. Sci,* 2012, **30**, 93.
56 J. I. Pankove, Optical processes in semiconductors, 1nd ed, 1971, Prentice Hall (New Jersy), p 34.
57 A. Shafiee, M. M. Salleh and M. Yahaya, *Sains Malays.*, 2011, **40**, 173.
58 V. Figá and Z. Essaidi, *J. Optoelectron. Adv. Mater.*, 2008, **10**, 3392.
59 D. C. Tiwari, R. Jain and S. Sharma, *J. Appl. Polym. Sci.*, 2008, **110**, 2328.
60 E. M. Girroto, W. A. Gazotti, C. F. Tormena and M-A. De Paoli, *Electrochim. Acta*, 2002, **47**, 1351.
61 J. Zhang, J. P. Tu, D. Zhang, Y. Q. Qiao, X. H. Xia, X. I. Wang and Ch. D. Gu, *J. Mater. Chem.*,2011, **21**, 17316.
62 B. Yigitsoy, S. Varis, C. Tanyeli, I. M. Akhmedov and L. Toppare, *Electrochim. Acta,* 2007, **52**, 6561.
63 J. L. Bredas, J. C. Scott, K. Yakushi and G. B. Street, *Phys. Rev. B*, 1984, **30**, 1023.
64 M. J. L. Santos, A. G. Brolo and E. M. Girotto, *Electrochim. Acta*, 2007, **52**, 6141.